Available online at www.sciencedirect.com
ScienceDirect
Ceramics International 34 (2008) 285–292
CERAMICS INTERNATIONAL
www.elsevier.com/locate/ceramint

Characterization and in vitro application of nano-crystalline calcia stabilized zirconia (CSZ)/copolymer composites

Khaled R. Mohamed *, Emad El-Meliegy

National Research Centre, Biomaterials Department, Behoos St., Dokki, Cairo, Egypt

Received 29 November 2005; received in revised form 31 August 2006; accepted 26 September 2006
Available online 8 December 2006

Abstract

The ideal implant should have long stable life in the physiological environment and induce natural bone growth around implants. In this study, nano-sized particles of calcia stabilized zirconia (CSZ) was used as a filler in poly(hydroxyethylmethacrylate–methylmethacrylate) p(HEMA–MMA) grafted onto chitosan copolymer to produce a bioactive composites analogous to bone. Results coming from this study confirmed that the grafting percentage of CSZ–copolymer composite was enhanced compared to the copolymer as a result of nano-sized filler. Thermo-gravimetric analysis (TGA) proved the presence of attached copolymer layer onto the filler particles for CSZ–copolymer composite. Swelling properties was reduced for CSZ–copolymer composite proving the stability and lower affinity of this composite to water molecules. In vitro tests indicate that the adsorption of calcium ions (Ca^{2+}) and phosphate ions (PO_4^{3-}) on the surface of the composites are enhanced. That was confirmed by the formation of a bone-like apatite layer. Fourier transformer infrared spectrophotometer (FT-IR) post-immersion confirmed the formation of carbonate-apatite layer onto the surface of the copolymer and CSZ–copolymer composite at 3 and 21 days, respectively. SEM post-immersion showed enhanced bone-like apatite layer (calcium-phosphate layer) onto the CSZ–polymer composite compared to the copolymer. Subsequently, the formation of a bone-like apatite layer is found to be controlled by the change in content of CSZ filler.

Keywords: CSZ; Chitosan; HEMA; Bioactive composites; In vitro

1. Introduction

Advanced ceramic materials offer many attractive physical, biological and mechanical properties to be used in a growing variety of medical applications. However, ceramics, without exception, are stiff, hard and brittle solids. Zirconia is being developed because of the improved mechanical properties, but there are still contradicting results coming from the phase transformation which are more complex than for alumina. The association of two ceramic materials can lead to new materials which can be two phase ceramic matrix composites, such as (Al_2O_3–ZrO_2) [1].

Zirconia can be a substitute to alumina for the ceramic ball heads of hip prostheses, because of its higher fracture toughness [2]. The zirconia–alumina system (ZA; 80 wt.% ZrO_2–20 wt.% Al_2O_3) is well known for its high flexural strength and is classified as a bio-inert ceramic [3]. Calcia (12 mol%) stabilized zirconia (CSZ) powders showed the coexistence of monoclinic and cubic solid solutions between 1180 and 1325 °C [4]. The bioceramic 3 mol% yttria stabilized zirconia (3Y-TZP) has good potential as a material for femoral head replacement due to its high wear resistance and excellent biocompatibility [5].

Although, many polymeric materials have been successfully inserted into the human body as substitutes for both hard and soft tissues, they always do not serve all needs of implant operations. On the other hand, because polymers are relatively radiolucent, implanted polymers are practically undetectable by X-rays [6]. To improve the biocompatibility of polymeric implant materials, other fillers have been used.

Acrylic bone cement is the only biomaterial that is currently used for anchoring prosthesis to the contiguous bone in cemented arthroplastics. Increasing the mechanical properties and the bioactivity of surgical cement, the linkage of two monomers, hydroxyethylmethacrylate (HEMA) and methylmethacrylate (MMA), by copolymerization to a modified

* Corresponding author.
E-mail address: Kh_rezk@yahoo.com (K.R. Mohamed).

0272-8842/$34.00
doi:10.1016/j.ceramint.2006.09.022

apatite was reported [7]. Chitosan, biocompatible, biodegradable, non-toxic, improves osseous healing of defects in femoral coundyl of sheep and stimulate cell proliferation and organized the hystoarchitectural tissue structure [8]. Previous work applied the grafting technique to modify the mechanical properties of poly-HEMA [9].

It is known that the properties composites can be sometimes higher than the same properties of each of the individual materials, when taken separately [1]. From the physical and biological stand points, ZrO_2 is the radiopaque filler of choice to be incorporated in pMMA implant material and addition of TCP could improve its biocompatibility [6]. Zirconia has high stiffness and toughness properties compared to hydroxyapatite and it has also been incorporated in resin bone cement to act as radiopaque filler [10]. ZrO_2 and pMMA particles increase proliferation and alkaline phosphatase specific activity and Al_2O_3, ZrO_2 and pMMA particles elicit direct effects on osteoblasts and that cell response depends on the particle type [11]. Taking into account the X-ray opacity, mechanical strength, water absorption and biocompatibility, the pMMA composite containing ZrO_2 appears to be a very promising material for implants [6].

Recent studies have shown that the addition of radiopaque agents in pMMA enhance macrophage–osteoclast differentiation and therefore may contribute to bone resorption which can ultimately lead to loosing of the prosthesis [12]. Mechanical evaluations of bioactive ceramic coatings on bio-inert metallic substrates have brought worldwide attention in both orthopedic and dental applications. To bridge the gap in ceramic coatings having poor mechanical properties, bioceramic composite coatings are being developed [13].

The material must be able to tolerate the hostile environment within the body in addition to the cyclic loads imposed upon it during gait. It is therefore critically important to establish the materials long-term performance under cyclic loading within SBF environment [5]. Kokubo et al. [25] showed that the formation of bone-like apatite is induced by functional groups on the materials, such as Zr–OH, Si–OH and Ti–OH that have a specific arrangement. These functional groups in the body environment assume a negative charge and finally induce bone-like apatite formation.

The aim of the work deals with the improvement of bioactivity of bio-inert nano-size of calcia partially stabilized zirconia particles via its impregnation into p(HEMA–MMA) grafted chitosan copolymer to be used as coating layer onto the metallic shaft of hip prostheses. The copolymer and CSZ composite samples are prepared, characterized and followed in freshly prepared SBF up to 28 days to confirm the formation of bone-like apatite layer on their surfaces.

2. Materials and methods

2.1. Starting materials

Calcia partially stabilized zirconia powder (size < 100 nm) was prepared via polymeric route according to Moustafa [4]. Chitosan polymer (high molecular weight and Brookfield viscosity: 800,000 cps), 2-hydroxyethylmethacrylate, methylmethacrylate monomers were provided by (Alderich). Cerric ammonium nitrate (CAN) initiator was provided by (BDH Chemical Ltd., Poole, England) and glacial acetic acid was used to dissolve chitosan.

2.2. Preparation of copolymer samples

0.1 g of chitosan was dissolved in 3% acetic acid, 20% of HEMA and 10% of MMA monomers were added to chitosan solution, well mixed and then 0.1 g of CAN initiator was added to graft monomers onto chitosan polymer. The mixture was put in water bath at 40 °C for 3 h to achieve the copolymerization process. The copolymer mixture was left overnight at ambient temperature and then washed with a mixture of ethanol–acetone with stirring for 1 h to remove homopolymer. The mixture was filtered then collected and dried at 60 °C for 24 h. The grafting ($G\%$) is calculated according to the following equation [14]:

$$G\% = \frac{W - W_0}{W_0} \times 100$$

where W is the weight of grafted chitosan and W_0 is the weight of original chitosan.

2.3. Preparation of composite samples

Fixed weight (1 g) from nano-sized CSZ powder was well mixed with the copolymer mixture after 2.5 h from copolymerization process and kept at 40 °C in water bath for 30 min. The CSZ copolymer composite was left overnight at ambient temperature and then the mixture was washed with a mixture of ethanol–acetone with stirring for 1 h to remove homopolymer. The mixture was filtered, collected and dried at 60 °C overnight. The grafting of copolymer in the presence of filler (CSZ powder) was calculated according to the following equation:

$$G\% = \frac{W_1 - W_0}{W_0} \times 100$$

where W_1 is the weight of grafted chitosan in the presence of 1 g of filler and W_0 is the weight of original chitosan.

2.4. Characterization of samples

The phase purity of samples was examined by X-ray diffractometer Diana Corporation (USA) equipped with Co Kα radiation, $\lambda = 1.79026$ Å with Fe filter.

The thermo-gravimetric analysis of the prepared samples was carried out using a Perkin-Elmer (USA) thermo-gravimetric analyzer in air. The measurements were performed in air with a heating rate of 10 °C/min within the temperature range of 50–1000 °C.

The infrared spectra of the prepared samples were obtained in the range 4000–400 cm^{-1} using KBr technique by using Fourier transformer infrared spectrophotometer (FT-IR) NEXAS 670, Nicolet, USA.

The morphology of the prepared samples was examined with a JXA 840A Electron Probe Microanalyzer (JEOL, Japan). The

scanning electron microscope measurement for each sample was carried out at different magnification.

2.5. Water absorption ability

Water absorption (W.A.%) studies are of great importance for biodegradable materials, because when implanted, it will inevitably be in the presence of the body fluids that will diffuse into the bulk of the polymer as degradation is taking place. For W.A. measurements, all the samples were weighted before being immersed in SBF at pH 7.4 and body temperature ($T = 37\ ^\circ C$) [15]. After immersion for different periods, the samples were carefully removed from the SBF containing tubes and immediately weighted for the determination of the wet weight as a function of the immersion time. W.A.% is given by the following equation:

$$\text{W.A.}\% = \frac{W_f - W_i}{W_i} \times 100$$

where W_i is the initial weight of the sample and W_f is the final weight after a given time of immersion.

2.6. In vitro bioactivity test

Standard in vitro bioactivity test was carried out to evaluate the formation (or not) of an apatite layer on the surface of the copolymer and composites samples. In order to study the bioactivity, samples were soaked in SBF, proposed by Kokubo et al. [16] at 37 °C and pH 7.4 for several periods of times up to 28 days [17]. The SBF has a composition similar to human blood plasma and has been extensively used for in vitro bioactivity tests [18]. After immersion, the specimens were removed from the SBF solution and were abundantly rinsed with deionized distilled water in order to remove the soluble inorganic salts and to stop the reaction. Total calcium and phosphate ions were measured in SBF after withdrawl the samples spectrophotometrically at $\lambda = 602\ cm^{-1}$ for calcium ions and at $\lambda = 575\ cm^{-1}$ for phosphorus ions using biochemical kits.

2.7. Characterization of samples after withdrawl from SBF

FT-IR analysis was also carried out for the samples pre- and post-immersion to confirm the formation of apatite layer onto the surface. The dried copolymer and CSZ composite samples were analyzed pre- and post-immersion 21 days in SBF using scanning electron microscopy (SEM). For SEM the substrates were mounted on metal stubs, and coated with gold before examination.

3. Results and discussion

3.1. The grafting percentage

The grafting percentage was 2524 and 3531 for copolymer and CSZ composite samples, respectively. This proves that the presence of filler particles enhanced the grafting % confirming high affinity of nano-size structure of filler to the copolymer.

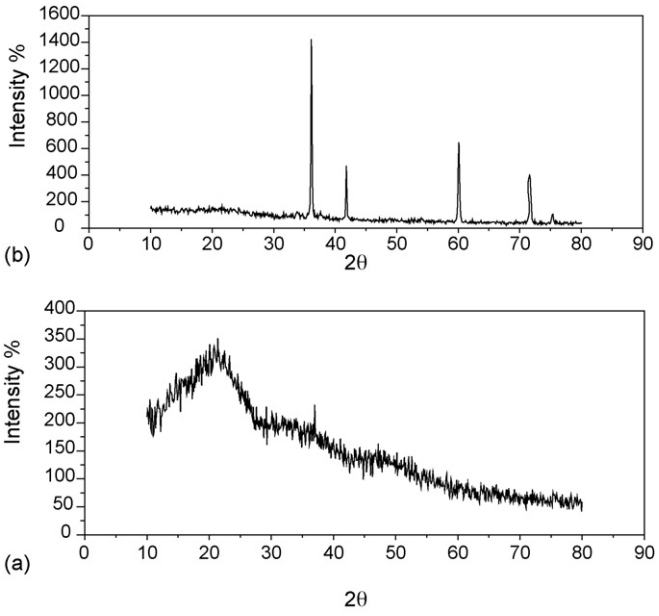

Fig. 1. XRD spectra of: (a) copolymer and (b) CSZ composite.

3.2. Phase analysis

The XRD patterns of copolymer and CSZ composite samples are shown in Fig. 1. In case of copolymer sample, there was hump (broad peak) in the range of 2θ (12–25°) at maximum d (Å) = 4.82 which was shifted from d (Å) = 4.37 characterizing chitosan structure (JCPDS, Card No. 39-1894). The result proves the interaction between polymer and monomer forming the copolymer structure.

For CSZ composite, the hump peak of copolymer was completely disappeared in the composite sample denoting effect of filler on the copolymer and amorphous structure of copolymer. The characteristic peaks, which are due to the presence of mixture of cubic phases, are still present in the composite at d-spacing (Å) 2.88, 2.50, 1.78, 1.52 and 1.46 with lower intensities. These d-spacing values were shifted from patterns of CSZ powder as following: 2.96, 2.56, 1.81, 1.54 and 1.48, respectively (JCPDS, Card No. 26-341). This proves coating effect onto the filler particles and some interaction.

3.3. FT-IR analysis

FT-IR spectrum of copolymer sample is shown in Fig. 2a. The band appeared at 3448 cm^{-1} is assigned to OH^- group characterizing structure of chitosan and pHEMA structure denoting grafting process. The bands at 519 and 900, 1457 and 2923, and 1384 cm^{-1} are assigned to CH, CH_2 and CH_3, respectively. Also, two bands at 850 and 750 cm^{-1} are assigned to pMMA and/or CH out of plane band [15]. Additionally, the bands at range of 1023–1157, 1276 and 1726 cm^{-1} are assigned to C–O, CCO and C=O groups, respectively, characterizing the copolymer structure. The band at 1650 cm^{-1} is assigned to amide I which characterizes chitosan structure [19].

FT-IR spectra of CSZ powder and its composite with copolymer are shown in Fig. 2b and c, respectively. No

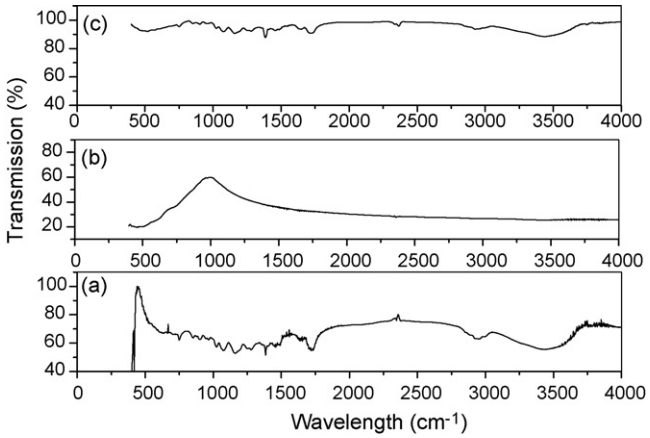

Fig. 2. FT-IR spectra of: (a) copolymer, (b) CSZ powder and (c) CSZ composite.

characteristic bands appeared for powder as in Fig. 2b. The characteristic bands for copolymer structure, such as CH, CH_2 and CH_3, C–O, CCO, C═O and amide are still appeared in spectrum of the composite. Also, they had lower optical density (O.D.) compared to the original copolymer sample proving effect of filler on these sites, such as O.D. of OH^- reduced from 0.252 to 0.056, CH or OH^- from 0.20 to 0.03, C═O from 0.26 to 0.046, CH_3 from 0.272 to 0.061, C–O from 0.264 to 0.041 and CH from 0.20 to 0.02, respectively (Fig. 2c).

3.4. Thermal analysis

The thermo-gravimetric analysis (TGA) of CSZ powder, copolymer and CSZ composite samples are shown in Fig. 3. The TGA of copolymer had three successive weight losses. The first weight loss recorded 6.32% at 214 °C due to release of absorbed water. The destruction of copolymer started with temperature rise and continued up to 393 °C with weight loss 83.57%. The destruction was accompanied by the evolution of CO_2, NH_3 and H_2O molecules [20]. The last weight loss 9.82% was recorded at 450 °C due to the rest of organic materials (Fig. 3a).

TGA of CSZ powder had very low weight loss 0.39% as a result of the release of absorbed water molecules from the

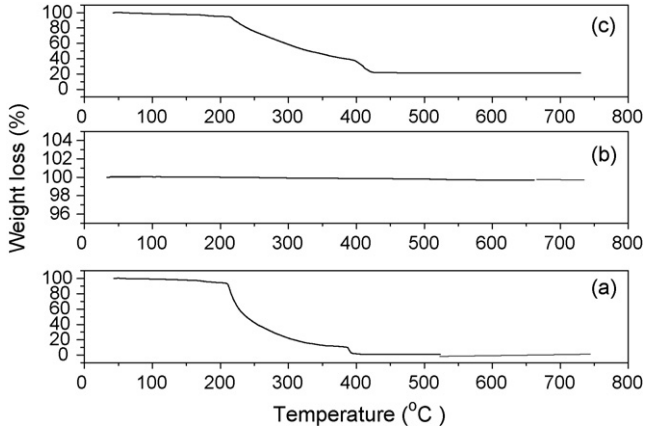

Fig. 3. TGA of: (a) copolymer, (b) CSZ powder and (c) CSZ composite.

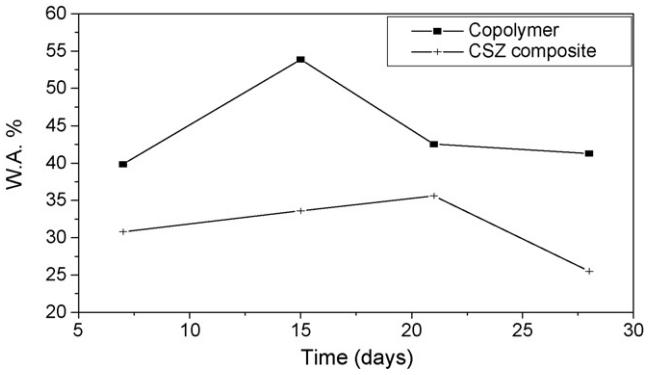

Fig. 4. Water absorption (W.A.) of copolymer and CSZ composite in SBF for different periods.

surface of particles confirming the stability of powder, as it was prepared at high temperature (Fig. 3b). The TGA of CSZ composite had three successive weight losses. The first step recorded 5.37% at 211 °C due to the release of absorbed water molecules. The second step is 56.87%, corresponding to the destruction of composite started after 211 °C and continued up to 396 °C with the release of NH_3, CO_2 and water molecules. In the third step, weight loss was 16.73% at nearly 450 °C due to the release of rest of organic materials (Fig. 3c). The total loss in weight was 78.98%. Therefore, the attached copolymer onto the particle surface was 78.69%, which is calculated by subtracting the weight loss of CSZ powder (0.39%) from the weight loss of CSZ composite (78.98%). This confirmed the presence of copolymer layer attached onto the surface of filler particles proving the coating and compatibility between two matrices.

3.5. Water absorption

The water absorption versus time for copolymer and CSZ composite samples is shown in Fig. 4. The W.A. values for copolymer samples at all periods were higher compared to CSZ composite samples. This proves that hydrophilic behavior (swelling) is mainly a result of the presence of –OH groups in the copolymer structure which has high affinity to water molecules. While lower hydrophilicity and stability of CSZ composite samples in SBF may result from the presence of filler particles, which affected OH sites of the copolymer.

3.6. In vitro behavior

The concentration of Ca^{2+} ions in SBF after immersion of copolymer sample at all periods except at 3 days was lower than that of control proving deposition of Ca^{2+} ions onto the surface of copolymer especially at 7 and 21 days (Fig. 5). In this domain, the chitosan forms a water insoluble gel in the presence of Ca^{2+} ions presenting pharmacologically beneficial effects on osteoconductivity [21]. For CSZ composite samples, Ca^{2+} ion concentrations in SBF after immersion at all periods were lower compared to these in control and copolymer sample especially at 15 days. This proves that the presence of filler particles

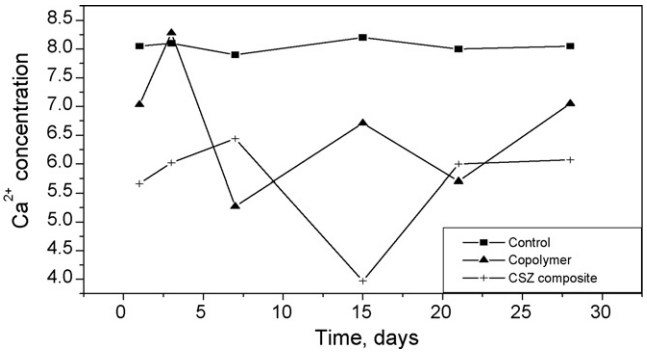

Fig. 5. Total calcium ions (Ca^{2+}) concentration pre- and post-immersion of copolymer and CSZ composite in SBF for different periods compared to SBF as control. Standard errors for Ca^{2+} ions concentration are shown in Table 1.

Table 1
Standard errors (%) of total calcium ions concentration (Ca^{2+}) for the tested sample ($n = 3$)

	Period (days)					
	1	3	7	15	21	28
Control	0.11	0.1	0.1	0.2	0.1	0.2
Copolymer	0.416	0.61	0.264	0.6	0.1	0.8
CSZ composite	0.3	0.2	0.4	2	0.2	0.2

within the composite enhanced the adsorption of Ca^{2+} ions on its surface inspite of the filler contains calcium in its structure; hence this is in the favor of the formation of bone-like apatite layer on the composite surface (Table 1).

The concentration of phosphate ions (PO_4^{3-}) in SBF after immersion at all periods for copolymer and CSZ composite samples were lower than that of control especially at longer time, such as 15, 21 and 28 days (Fig. 6). This shows that deposition of PO_4^{3-} ions from fluid on the sample surface was achieved especially for copolymer sample, this behavior coincided with Wang et al. [22] who proved that the presence of affinity for chitosan as cationic polymer to phosphate ions. Therefore, from the results of the in vitro test, it is notified that the formation of calcium phosphate (apatite) onto the surface of copolymer or CSZ composite could be expected. These results

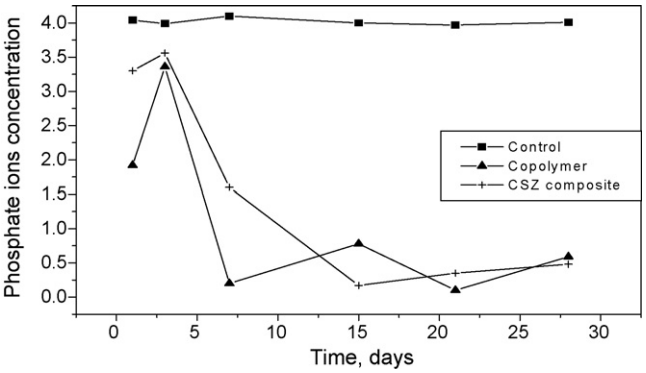

Fig. 6. Phosphate ions (PO_4^{3-}) concentration pre- and post-immersion of copolymer and CSZ composite in SBF for different periods compared to SBF as control. Standard errors for PO_4^{3-} ions concentration are shown in Table 2.

Table 2
Standard errors (%) of phosphate ions concentration (PO_4^{3-}) for the tested sample ($n = 3$)

	Period (days)					
	1	3	7	15	21	28
Control	0.1	0.1	0.2	0.1	0.1	0.1
Copolymer	0.1	0.5	0.1	0.2	0.05	0.2
CSZ composite	0.2	0.4	0.4	0.03	0.2	0.2

are coincided with those who reported that calcium phosphate formed either on or underneath the surface of copolymer depending on the pH of phosphate solution [23] (Table 2).

3.7. Solid characterization of samples after withdrawl from SBF

3.7.1. FT-IR analysis

The FT-IR results of copolymer samples pre- and post-immersion are shown in Fig. 7. The O.D. of –OH group at 3429 cm^{-1} and amide at 1629 cm^{-1} were highly increased post-immersion (3 days) compared to pre-immersion from 0.222 to 0.753 and 0.222 to 0.450, respectively, proving biolayer formation. Then, their values were reduced after longer time proving their involvement in the biolayer or their masking. The O.D. of CH_3 and CH_2 and/or N–H stretching bands appeared at 1384 and 2952 cm^{-1}, respectively, were enhanced post-immersion compared to pre-immersion from 0.27 to 0.49 and 0.20 to 0.65, respectively, proving effect of immersion. Also, the O.D. of C–O, C=O and CCO groups at 1159, 1723 and 1278 cm^{-1} were highly enhanced post-immersion especially at 3 days from 0.28 to 0.53, 0.26 to 0.58 and 0.256 to 0.51, respectively. Consequently, these values decreased after longer time proving deposition of some ions and its release into the media or its involvement in the biolayer structure.

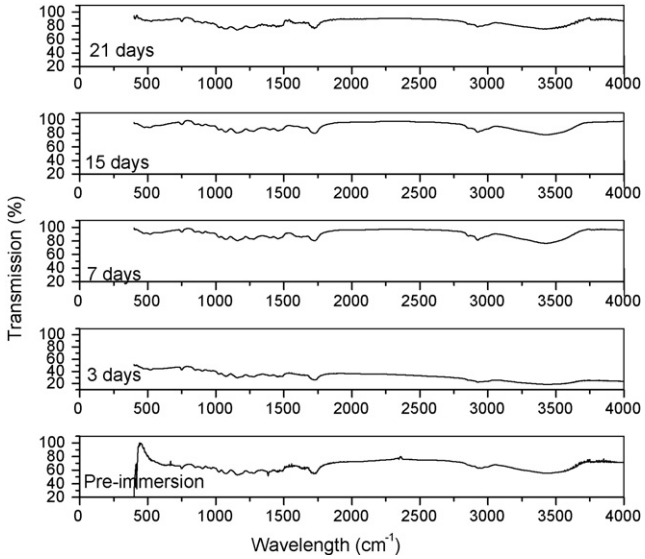

Fig. 7. FT-IR spectra of copolymer pre- and post-immersion for different periods.

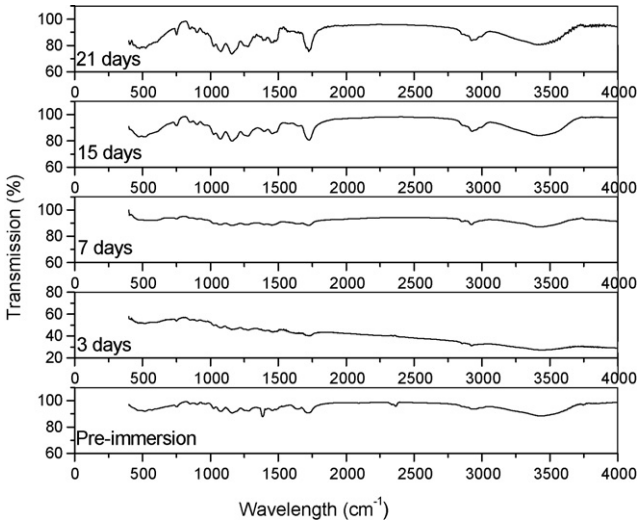

Fig. 8. FT-IR spectra of CSZ composite pre- and post-immersion for different periods.

Additionally, the O.D. of CH and/or bending PO_4^{3-} at 901, 519 and 417 cm^{-1} and C–O and/or stretching PO_4^{3-} at 1150, 1075 and 1024 cm^{-1} were highly increased especially at 3 days post-immersion compared to pre-immersion and after longer time of soaking. This proves deposition of phosphate ions on the surface then its release into the media or its involvement in the biolayer. This is coincided with biochemical data. Also, the O.D. of CH_2 and/or stretching carbonate group at 1459 and 1400 cm^{-1} and CH and/or bending carbonate group at 850 and 750 cm^{-1} was enhanced post-immersion especially at 3 days proving deposition of some ions onto the copolymer surface. This result is in favor of the formation of carbonated apatite layer. After longer time, the O.D. of these bands was reduced compared to pre-immersion and 3 days denoting their involvement in the biolayer formation or its release into the media The FT-IR results of the CSZ composite samples pre- and post-immersion are shown in Fig. 8. The O.D. of –OH group at 3428 cm^{-1} and amide group at 1630 cm^{-1} were enhanced post-immersion at all periods especially at 21 days compared to pre-immersion proving formation of biolayer [24]. Also, the O.D. of CH_3 and CH_2 and/or N–H groups at 1384 and

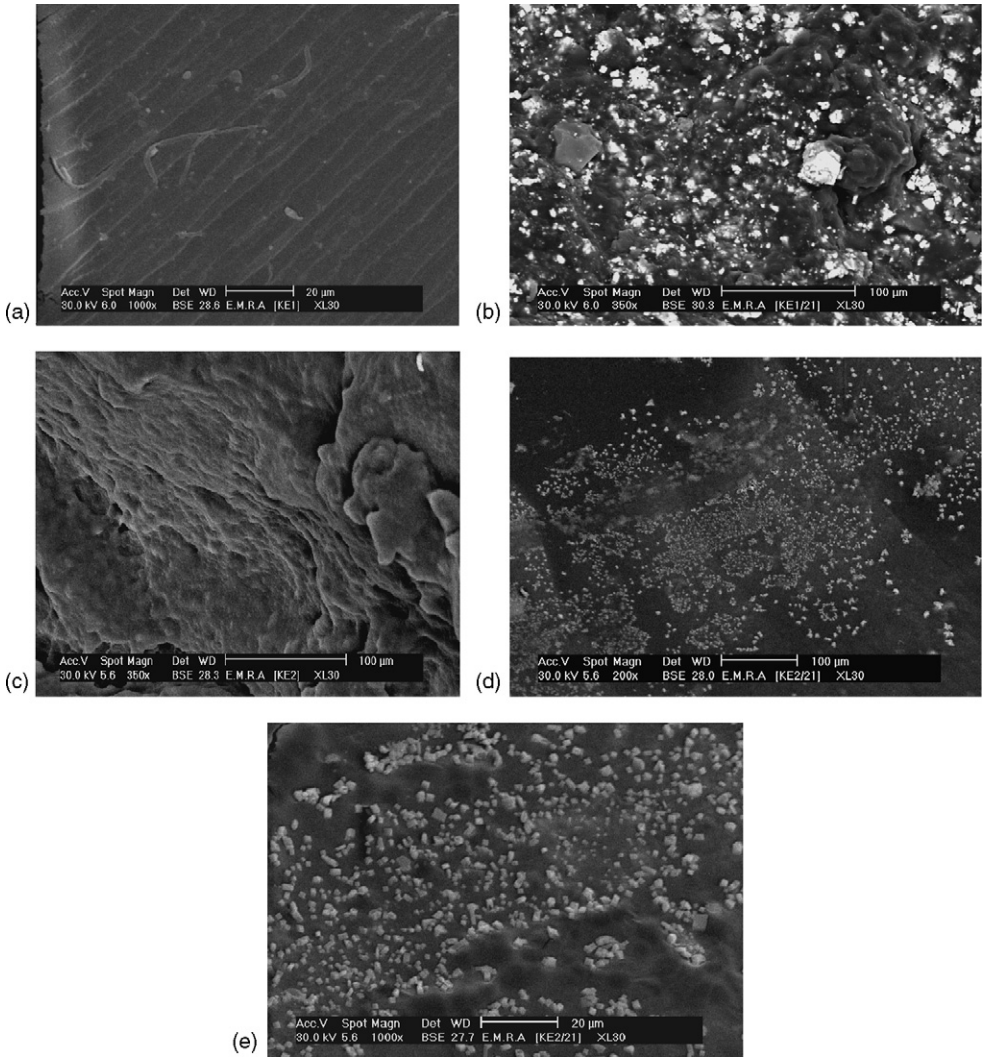

Fig. 9. SEM of copolymer and CSZ composite pre- and post-immersion in SBF for 21 days.

2925 cm^{-1} were enhanced post-immersion especially at 21 days compared to pre-immersion. Also, the O.D. of C–O, C=O and CCO groups were increased post-immersion compared to pre-immersion from 0.046 to 0.137, 0.046 to 0.125 and 0.03 to 0.102, respectively, proving their involvement in biolayer or deposition of some ions on the surface of composite.

Additionally, the O.D. of CH and/or bending PO_4^{3-} at 900, 516 and 492 cm^{-1} and C–O and/or stretching PO_4^{3-} at 1150, 1076 and 1024 cm^{-1} were gradually increased post-immersion till 21 days recording a maximum values proving deposition of phosphate ions on the surface and forming apatite layer. These results are coincided with biochemical data. Also, the O.D. of CH_2 and/or stretching carbonate group at 1459 cm^{-1} and CH and/or bending carbonate group at 850 and 750 cm^{-1} were enhanced post-immersion especially at 21 days denoting effect of deposition of carbonate ions from SBF onto the composite surface. This proves that the presence of CSZ filler in the copolymer enhanced the formation of apatite layer onto the surface of composite compared to copolymer samples especially after longer time and prevent the release of deposited ions into the media. This result coincided with those reported that zirconia form apatite on its surface in SBF as the presence of Zr–OH group that is effective for apatite nucleation [25].

3.7.2. Surface morphology

SEM of copolymer and CSZ composite samples are shown in Fig. 9. For copolymer sample, pre-immersion, it shows the presence of smooth surface with longitudinal lines indicating formation of copolymer (Fig. 9a). Post-immersion, it indicates the presence of many particles with brightness color on the surface denoting deposition of ions onto the copolymer surface (Fig. 9b).

For CSZ composite, pre-immersion, SEM shows the presence of smooth and rough surfaces proving coating and homogeneity between two matrices (filler and copolymer) (Fig. 9c). Post-immersion, it shows the presence many particles on the composite surface proving deposition of ions, which confirmed the formation of a bone-like apatite layer on its surface (Fig. 9d and e).

4. Conclusions

(1) The grafting % of CSZ composite was enhanced compared to the copolymer as a result of nano-sized filler.
(2) Swelling properties was reduced for CSZ composite proving stability of composite and lower affinity to water molecules into SBF denoting effect of filler. As concerns in vitro bioactivity, the adsorption of Ca^{2+} and PO_4^{3-} ions on CSZ composite surface was enhanced as confirmed by the addition of CSZ particles followed by the formation of a bone-like apatite layer.
(3) FT-IR post-immersion confirmed the formation of carbonated-apatite layer onto the surface of the copolymer and CSZ composite at 3 and 21 days, respectively. SEM post-immersion showed enhanced a bone-like apatite layer (calcium-phosphate layer) onto the CSZ composite compared to the copolymer. SEM post-immersion showed enhanced a bone-like apatite layer (calcium-phosphate layer) onto the CSZ composite compared to the copolymer. Subsequently, the formation of apatite layer is found to be controlled by the change content of CSZ filler containing effective functional group (Zr–OH) for apatite nucleation.

References

[1] J. Rieu, P. Goeuriot, Ceramic composites for biomedical applications, Clin. Mater. 12 (1993) 211–217.
[2] P. Christle, J.M. Dorlot, A. Meunier, On the specification for the use of bioceramics in total hip replacements, in: H. Oonishi, K. Aoki (Eds.), Bioceramics, vol. 1, Sawai Ishiyaku Euro-America, Tpkio, MO, 1989 pp. 266–271.
[3] K. Tsukuma, K. Ueda, M. Shimada, Strength and fracture toughness of isostatically hot-pressed composites of Al_2O_3 and Y_2O_3 partially stabilized ZrO_2 tetragonal ZrO_2, J. Am. Ceram. Soc. 68 (1) (1965) C4.
[4] E. Moustafa, Ca–PSZ prepared via polymeric sol–gel route, Ceram. Int. 26 (2) (2000) 215–220.
[5] B.J. Hulm, W.J. Evans, Evaluation of the cyclic fatigue lifeof 3 mol% yttria stabilized Zirconia bioceramic using biaxial flexion, J. Am. Ceram. Soc. 83 (2) (2000) 321–328.
[6] P.-I. Chang, Polymer implant materials with improved X-ray opacity and biocompayability, Biomaterials 2 (3) (1981) 151–155.
[7] V. Delpech, A. Lebugle, Calcium Phosphate and interfaces in orthopedic cement, Clin. Mater. 5 (1990) 209–216.
[8] R.A. Muzzarelli, M. Mattioli-Belmonte, C. Tietz, et al., Stimulatory effect on bone formation exerted by a modified chitosan, Biomater. J. 15 (13) (1994) 1075–1081.
[9] G.H. Hsiue, J.M. Yang, R.L. Wu, Preparation and properties of a biomaterial: HEMA grafted SBS by γ-ray irradiation, J. Biomed. Mater. Res. 22 (5) (1988) 405–415.
[10] R.P. Kusy, J. Biomed. Mater. Res. 12 (1978) 275–305.
[11] H.C. Lohmann, D.D. Dean, G. Koster, D. Casasola, G.H. Buchhorn, U. Fink, Z. Schwartz, B.D. Boyan, Ceramic and PMMA particles differentially affect osteoblast phenotype, Biomaterials 23 (2001) 1855–1863.
[12] A. Sabokbar, Y. Fujikawa, D.W. Murray, N. Athanasou, Radioopaque agents in bone cement increase bone resorption, J. Bone Joint Surg. Br. 79B (1997) 22, 129.
[13] L. Fu, K.A. Khor, J.P. Lim, Surf. Coat. Technol. 127 (2000) 66.
[14] A. Lagos, J. Reyes, Grafting onto chitosan. I. Graft copolymerization of methylmethacrylate onto chitosan with Fenton's Reagent (Fe^{2+}–H_2O) as a redox initiator, J. Polym. Sci. 26 (1988) 985–991.
[15] A.L. Oliveira, P.B. Malafaya, R.L. Reis, Sodium silicate gel as precursor for the in vitro nucleation and growth of a bone-like apatite coating in compact and porous polymeric structures, Biomaterials 24 (2003) 2575–2584.
[16] T. Kokubo, H.M. Kim, M. Kawashita, H. Takadama, T. Miyazaki, M. Uchida, T. Nakamure, Nucleation and growth of apatite on amorphous phases in simulated body fluid, Glastech. Ber. Glass Sci. Technol. 73 (2001) 247–254.
[17] Q.Q. Qiu, P. Ducheyne, P.S. Ayyaswamy, New bioactive, degradable composite microspheres as tissue engineering substrates, J. Biomed. Mater. Res. 52 (1) (2000) 66–76.
[18] I.B. Leonor, R.A. Sousa, A.M. Cunha, R.L. Reis, Z.P. Zhong, D. Greenspan, Novel starch thermoplasatic/bioglass composites: mechanical properties, degradation behavior and in vitro bioactivity, J. Mater. Sci. Mater. Med. 13 (2002) 939–945.
[19] F. Chen, Z. Wang, C. Lin, Preparation and characterization of nano-sized HA particles and HA/Chitosan nano-composite for use in biomedical materials, Mater. Lett. 57 (2002) 858–861.
[20] N. Angelova, N. Manolova, I.J. Rashikov, Bioactive Compatible Polym. 10 (1995) 10.
[21] M.R. Finisie, A. Josue, V.T. Favere, M.C. Laranjeira, Synthesis of calcium phosphate and chitosan bioceramics for bone regeneration, An-Acad-Bras-Clienc. 73 (4) (2001) 525–532.

[22] X. Wang, J. Ma, Y. Wang, H. Binglin, Structural characterization of phosphorylated chitosan and their applications as effective additives of calcium phosphate cements, J. Biomater. 22 (16) (2001) 2247–2255.
[23] M.L. Gaillard, I.R. Dewijn, C.A. Van Blitlerswijk, Calcium phosphate depositions in PEO/PBT copolymer prior to implantation, in: P. Ducheyne, D. Christiansen (Eds.), Bioceramic, vol. 6, Elsevier Science, PA, USA, 1993.
[24] G.E. El-Bassyouni, Assessment of biocompatibility of bone substitutes and their decalcification, Ph.D. Thesis, Biophysics Department, Faculty of Science, Cairo University, Egypt, 1999.
[25] T. Kokubo, H. Kim, M. Kawashita, Novel bioactive materials with different mechanical properties, Biomaterial 24 (2003) 2161–2175.